Hany Ghoneim
Department of Mechanical and Industrial Engineering
Kuwait University
PO Box 5969, Safat 13060
Kuwait

Fluid Surface Damping: A Technique for Vibration Suppression of Beams

A fluid surface damping (FSD) technique for vibration suppression of beamlikestructures is proposed. The technique is a modification of the surface layer damping method. Two viscoelastic surface layers containing fluid-filled cavities are attached symmetrically to the opposite surfaces of the beam. The cavities on one side are attached to the corresponding cavities on the other side via connection passages. As the beam vibrates, the fluid is pumped back and forth through the connecting passages. Therefore, in addition to the viscoelastic damping provided by the surface layers, the technique offers viscous damping due to the fluid flow through the passage. A mathematical model for the proposed technique is developed, normalized, and solved in the frequency domain to investigate the effect of various parameters on the vibration suppression of a cantilever beam. The steady-state frequency response for a base white-noise excitation is calculated at the beam's free tip and over a frequency range containing the first five resonant frequencies. The parameters investigated are the flow-through passage viscous resistance, the length and location of the layers, the hydraulic capacitance of the fluid-filled cavities, and inertia of the moving fluid (hydraulic inertance). Results indicate that the proposed technique has promising potential in the field of vibration suppression of beamlike structures. With two FSD elements, all peak vibration amplitudes can be well suppressed over the entire frequency spectrum studied.

INTRODUCTION

Vibration control of thin structures is of great importance to the automobile, aircraft, and space industries. The surface layer damping method has been used as a simple and reliable means of controlling the vibration of such structures (Nashif et al., 1985; Cremer et al., 1988). In particular, constrained layer damping (CLD) has been widely used because of the relatively high damping it provides (Harrison et al., 1994; Henze et al., 1990; Tomlinson, 1990). In this method a layer of a viscoelastic material is bonded to the surface of the structure and constrained by a stiff constraining layer. Upon vibration of the structure the viscoelastic layer deforms and dissipates the excessive energy of vibration of the structure. The method, although successful, is effective over a limited range of temperatures and frequencies. A viscous fluid layer has been utilized for vibration control of plates (Ingard and Akay, 1987). In this application, a thin layer of fluid is trapped between the plate and a rigid back block. Upon vibration of the plate, the fluid is pumped from regions of compression to regions of rarefaction. The energy required to overcome the friction drag on the fluid is supplied by the plate engendering the damping effect. The high sensitivity of the technique to the operating conditions and

Received 12 July 1995; Revised February 1996.
Shock and Vibration, Vol. 4, No. 5,6, pp. 295–304 (1997)
ISSN 1070-9622/97/$8.00 © 1997 IOS Press

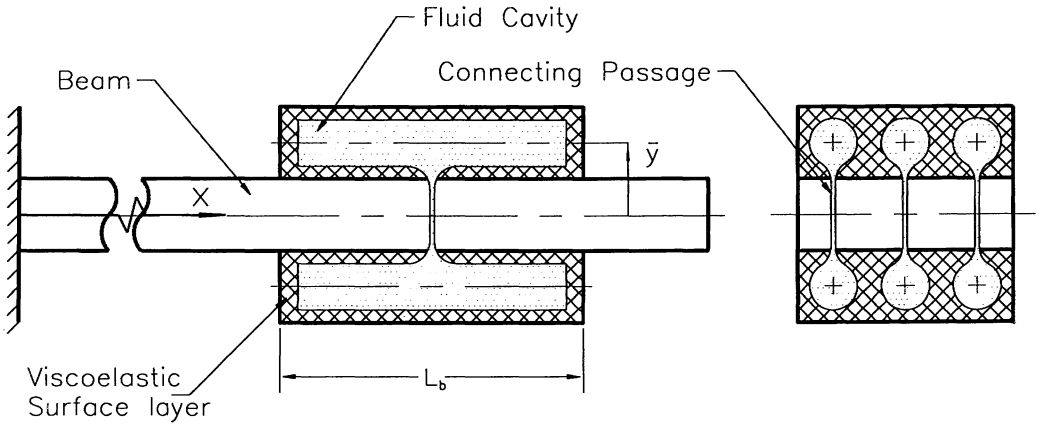

FIGURE 1 Schematic of a beamlike structure treated with a fluid surface damping element.

system parameters (Onsay, 1994) as well as the need for the backing block restricts the technique to very special applications.

Active control techniques have also been applied to control the vibration of thin structures. Active control using an electrorheological sandwiched beam was proposed and shown to reduce the transient response of the beam (Rahn and Joshi, 1994). The extreme high voltage required renders the technique impractical. Piezoelectric elements, used as actuators and/or sensors, were introduced for the active vibration control of beam- and platelike structures (Liao and Sung, 1991; Dosch et al., 1992; Hollkamp and Napolitano, 1994). These active techniques are more effective than the CLD method; however, unreliability, instability, complexity, and cost are some of the disadvantages that limit their use.

To overcome some of these disadvantages, hybrid techniques, which integrate the CLD into active control methods, were recently proposed. One such technique, the intelligent constrained layer (ICL), replaces the constraining layer of the CLD with a piezoelectric layer that acts as an actuator (Agnes and Napolitano, 1993; Nostrand et al., 1993; Shen, 1994). Baz and Ro (1993) introduced a modified ICL technique, active constrained layer damping (ACLD), in which an additional piezoelectric layer is sandwiched between the viscoelastic constrained layer and the structure. This additional piezoelectric layer acts as a sensor. The advantages of the modified technique over the conventional CLD were clearly demonstrated analytically and experimentally by Baz and Ro (1994) for a cantilever beam and over a considerable range of temperatures. Another hybrid technique was also proposed: Electromechanical surface damping (EMSD). This technique integrates the shunted piezoelectric damping method (introduced by Hagood and Von Flotow, 1991 into the CLD method). In this case the constraining layer of the conventional CLD is replaced by a shunted piezoelectric ceramic. Tuning the shunting piezoelectric circuit to one or more of the resonant frequencies of the structure renders a greater suppression of the resonant vibration amplitudes and/or a wider effective range of the vibration control as compared to the conventional CLD (Ghoneim, 1995).

In this article a simple, passive, and reliable technique for vibration suppression of beamlike structures is proposed, the fluid surface damping (FSD) technique. It is a modification of the surface layer damping method. A schematic of a FSD element applied to a beamlike structure is illustrated in Fig. 1, and the corresponding physical and hydraulic models that illustrate the fundamental working principal of the FSD element are presented in Fig. 2. Two viscolelastic surface layers containing fluid-filled cavities are attached symmetrically to the opposite surfaces of the beam. The cavities on one side of the beam's neutral axis are connected to the corresponding cavities on the opposite side via narrow passages. When the beam bends, the layer attached to one side of the beam contracts and the opposite layer stretches, causing the respective cavities to contract and expand and the fluid to be pumped from the contracting to the expanding cavities through the connecting passages as illustrated in Fig. 2. As the beam vibrates, the fluid is pumped back and forth through the connecting passages dissipating part of the excessive energy of vibration. Therefore, in addition to the viscoelastic damping provided by the surface layers, the technique offers viscous damping due to the fluid flow through the passages.

A rather simple mathematical model is proposed for the FSD portion of the treated beam. The model is normalized and solved, using the finite element, in the frequency domain in order to find the frequency

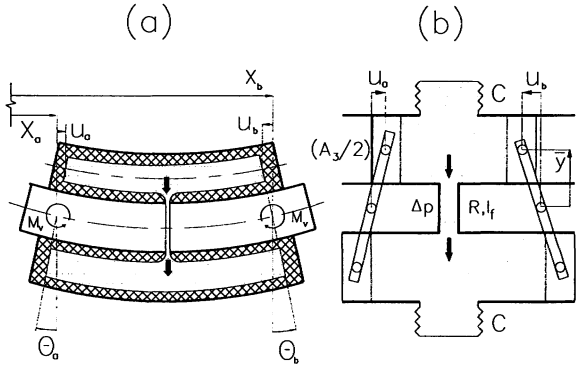

FIGURE 2 (a) Physical and (b) hydraulic models of the FSD element.

response of a cantilever beam subject to a white-noise displacement excitation at the base. A parametric study is conducted to investigate the effect of some parameters: the viscous resistance, length, and location of the viscoelastic layers; the hydraulic capacitance of the fluid-filled cavities; and the inertia of the moving fluid (hydraulic inertance). Results are discussed and the potential of the technique for the vibration suppression of beamlike structures is examined.

MATHEMATICAL MODEL

Basic Assumptions

Development of the governing equations for the FSD-treated portion of the beam is based on the following assumptions:

- small displacements and strains;
- perfect bonding between the surface viscoelastic layers and the beam;
- plane cross sections remain plane;
- all transverse displacements of all points of the surface layers and the beam on any cross section are the same and equal to the transverse displacement of the midplane of symmetry (i.e., no transverse normal strains);
- no axial loading and consequently the midplane of the beam does not experience any axial displacement;
- the initial axial displacement due to the fluid pressure inside the cavities is considered negligible;
- rotary inertia and shear deformation are negligible (Bernoulli–Euler beam);
- linear, isotropic, elastic material behavior for the beam and viscoelastic material behavior for the surface layer;
- incompressible, laminar flow;
- the pressure inside the cavities is uniform; that is, the pressure drop along the axes of the cavities due to the fluid flow inside the cavities is negligible; and
- viscous damping due to the fluid flow through the passage is the dominant source of hydraulic damping.

To satisfy the last two assumptions, some design consideration of the fluid circuit must be fulfilled. The hydraulic resistance of the connecting passage must be much larger than that of the cavities. That is l/d^4, where l and d respectively stand for the length and diameter, of the connecting passage must be much larger than that of the cavities. This would ensure that the pressure drop due to the axial flow inside the cavities is negligible compared to the pressure drop due to the flow through the connection passage. A connecting passage with a high slender ratio (length to diameter ratio) would also reduce the minor losses (exit and entrance losses) relative to the major one due to viscous damping. Well-rounded entrances at the connections between the passages and the cavities (Fig. 1) further reduce these minor losses and render the last assumption more realistic.

Governing Equations

Based on the above-mentioned assumptions and from the dynamic equilibrium of the differential element shown in Fig. 3, we have

$$-\frac{\partial^2 M}{\partial x^2} = \rho A \frac{\partial^2 w}{\partial t^2}, \tag{1}$$

where ρA is the mass per unit length of the composite beam ($\rho A = \sum \rho_i A_i$), w is the transverse displacement, and x is the axial coordinate. The bending moment M is

$$M = -\int_{A_1} \sigma y \, dA - \int_{A_2} \sigma y \, dA - \int_{A_3} (\Delta p/2) y \, dA$$
$$= E_1 I_1 \frac{\partial^2 w}{\partial x^2} + E_2 I_2 \otimes \frac{\partial^2 w}{\partial x^2} - \Delta p Q, \tag{2}$$

where σ is the axial stress; $E_1 I_1$ the flexure rigidity of the beam; E_2 the extensional-relaxation modulus of the surface layers' viscoelastic material; I_2 the moment of inertia of the surface layers' cross-sectional area, A_2, about the neutral axis of the beam; and Q the first moment of the fluid cavities' cross-sectional areas of one layer about the neutral axis, $Q = \int_{A_3/2} y \, dA = \bar{y} A_3/2$, with $\bar{y}$ being the perpendicular distance between the beam's neutral axis and the center line of

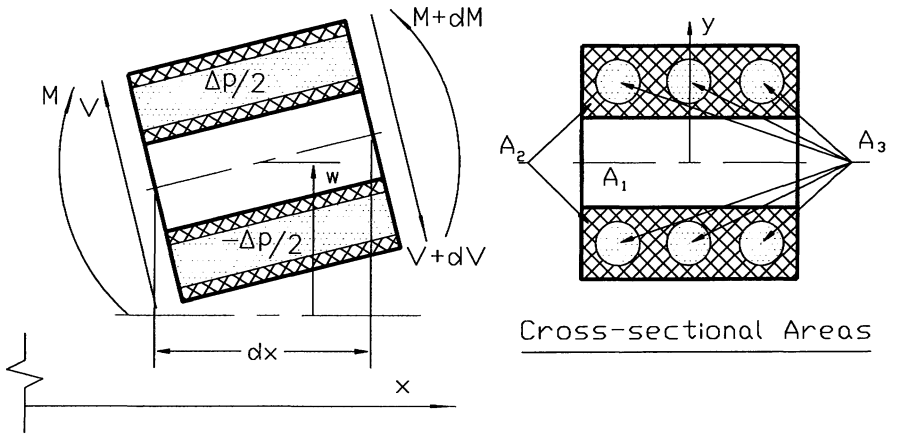

FIGURE 3 A differential element of the treated beam with an illustration of the different cross-sectional areas.

the cavity (Fig. 1). The cross-sectional areas A_1, A_2, and A_3 pertain to the beam, surface layers, and fluid cavities, respectively (Fig. 3). The symbol $\otimes$ stands for the heredity (Boltzmann) integrals (Christensen, 1982), $A \otimes B = \int_0^t A(t-\xi)(\partial B/\partial \xi)\, d\xi$. The pressure drop across the connecting passage, Δp, can be expressed as

$$\Delta p = K \otimes q, \tag{3}$$

where K is the equivalent hydraulic bulk-relaxation modulus of the fluid circuit [Fig. 2(b)] and q is the fluid volumetric flow induced by bending,

$$\begin{aligned} q &= (A_3/2)(u_a - u_b) \\ &= -(A_3/2)\bar{y}\{(\partial w/\partial x)_a - (\partial w/\partial x)_b\} \\ &= -Q(\theta_a - \theta_b) = -Q\Delta\theta, \end{aligned} \tag{4}$$

where u and θ are the average axial displacement and angular rotation of the surface layer's cross-sectional plane. The subscripts a and b designate the axial locations at which u and θ are measured, i.e., as shown in Fig. 2(a), at x_a and x_b, respectively. Substituting (3) and (4) into (2), we get

$$M = E_1 I_1 (\partial^2 w/\partial x^2) + E_2 I_2 \otimes (\partial^2 w/\partial x^2) + M_v, \tag{5}$$

where M_v is the hydraulic moment generated by the fluid circuit,

$$M_v = Q^2 (K \otimes \Delta\theta). \tag{6}$$

Substituting (5) and (6) into (1), we get the governing equation of the FSD-treated portion of the beam,

$$\begin{aligned} &\frac{\partial^2}{\partial x^2}\left\{E_1 I_1 \frac{\partial^2 w}{\partial x^2}\right\} + \frac{\partial^2}{\partial x^2}\left\{E_2 I_2 \otimes \frac{\partial^2 w}{\partial x^2}\right\} \\ &+ \rho A \frac{\partial^2 w}{\partial t^2} = 0, \end{aligned} \tag{7a}$$

noindent subject to

$$M(x_a) = -M_v \quad \text{and} \quad M(x_b) = M_v. \tag{7b}$$

Clearly, the problem of a beam treated with an FSD element is equivalent to the classical problem of a beam treated with a surface damping layer plus a couple of equal and opposite viscous moments, M_v, applied at both ends of the FSD element [Fig. 2(a)].

FREQUENCY ANALYSIS AND PARAMETRIC STUDY

Effect of the FSD treatment on the frequency response of a cantilever beam subjected to white-noise displacement excitation at the base was investigated. The response was found at the beam's free tip and over a wide range of frequencies covering the first five resonant frequencies. A parametric study was conducted to assess the impact of various parameters on the damping effectiveness of the technique as measured by the magnitude of the peak vibration amplitudes. The parameters considered in the current analysis were the viscous resistance R, the length and location of the FSD element, the hydraulic capacitance of the upper and lower cavities C, and the fluid inertia (hydraulic inertance) I_f. Nondimensional variables and parameters were adopted to facilitate the parametric study task.

In the frequency domain, the governing equations, Eq. (7), becomes

$$\frac{\partial^2}{\partial x^2}\left\{EI(\omega i)\frac{\partial^2 w_0}{\partial x^2}\right\} - \rho A \omega^2 w_0 = 0, \tag{8a}$$

subject to

$$M(x_a) = -M_v \quad \text{and} \quad M(x_b) = M_v,$$

where

$$M_v(\omega i) = Q^2 K^*(\omega i)\Delta\Theta. \tag{8b}$$

In (8) w_0 is the amplitude of the transverse displacement ($w = w_0 e^{i\omega t}$), Θ is the amplitude of the angular displacement ($\theta = \Theta e^{i\omega t}$), ω is the excitation frequency, and $EI(\omega i) = E_1 I_1 + E_2^*(\omega i) I_2$ where E_2^* is the complex Young's modulus of the surface layers' viscoelastic material. Based on the assumptions stated earlier and the hydraulic model shown in Fig. 2(b), the hydraulic complex bulk modulus, $K^*(\omega i)$, of the FSD element is

$$K^*(\omega i) = \frac{\Delta p}{q} = \frac{1}{C_e}\left\{\frac{-I_f\omega^2 + r\omega i}{-I_f\omega^2 + R\omega i + 1/C_e}\right\} = R\frac{-\frac{1}{\tau}\left(\frac{\omega}{\omega_n}\right)^2 + \omega i}{1 - \left(\frac{\omega}{\omega_n}\right)^2 + \tau\omega i}. \tag{9}$$

In the above equation τ is the hydraulic time constant ($\tau = RC_e$), ω_n is the hydraulic natural frequency ($\omega_n = 1/\sqrt{I_f C_e}$), and C_e is the equivalent hydraulic capacitance of the connected cavities ($C_e = C/2$, for identical cavities).

For the parametric study, the following nondimensional variables and parameters we adopted: X is the nondimensional axial coordinate, $X = x/L$; W is the nondimensional transverse displacement, w_0/L; $\widetilde{M}$ is the nondimensional bending moment, $\widetilde{M} = ML/E_1 I_1$; α is the nondimensional complex flexure rigidly, $\alpha = EI/E_1 I_1$; μ is the nondimensional mass per unit length, $\mu = \rho A/\rho_1 A_1$; Ω is the nondimensional frequency, $\Omega = \omega/\omega_0$; where L is the length of the beam and $\omega_0 = \sqrt{E_1 I_1/\rho_1 A_1 L^4}$. Notice that for the untreated portions of the beam, $\alpha = \mu = 1$. Upon normalization of the governing equation, Eq. (8), we get

$$\alpha\frac{\partial^4 W}{\partial X^4} - \mu\Omega^2 W = 0, \tag{10a}$$

subject to

$$\widetilde{M}(X_a) = -\widetilde{M}_v \quad \text{and} \quad \widetilde{M}(X_b) = \widetilde{M}_v,$$

where

$$\widetilde{M}_v = \widetilde{K}(\Omega i)\Delta\Theta. \tag{10b}$$

The nondimensional complex modulus, $\widetilde{K}(\Omega i)$, is expressed as

$$\widetilde{R}(\Omega i) = \widetilde{R}\left\{\frac{-\frac{1}{T}\left(\frac{\Omega}{\Omega_n}\right)^2 + \Omega i}{-1\left(\frac{\Omega}{\Omega_n}\right)^2 + T\Omega i}\right\}, \tag{11}$$

where $\widetilde{R}$ is the nondimensional hydraulic resistance of the connecting passages ($\widetilde{R} = RQ^2/\rho_1 A_1 L^3\omega_0$), T is the nondimensional time constant ($T = \tau\omega_0$), and Ω_n is the nondimensional natural frequency ($\Omega_n = \omega_n/\omega_0$).

RESULTS AND DISCUSSION

The frequency response of the treated cantilever beam was determined for different lengths and locations of the FSD element and for different values of $\widetilde{R}$, T, and Ω_n. Samples of the results are shown in Figures 4–11. The vertical axis in all these figures represents the amplitude ratio between the amplitude of the displacement response at the beam's free tip and the input displacement amplitude at the base. All numerical results were obtained over the frequency range $b = 0$–15, where $b = \sqrt{\Omega}$, that covers the first five natural frequencies, and for $\alpha = 1.25 + 0.25i$ and $\mu = 1.6$. The response was determined using the finite element method. Twenty beam elements with cubic Hermite shape functions (Reddy, 1993) were adopted in all the examples presented. The finite element results using 20 elements for the case shown in Fig. 4 are compared with the corresponding analytical ones using the program *Mathematica*, and excellent agreement was obtained. When displayed graphically, both results are indistinguishable and consequently the analytical results are not presented.

The introduction of the nondimensional variable b enhances the frequency response displayed in the figures and allows a direct comparison between the finite

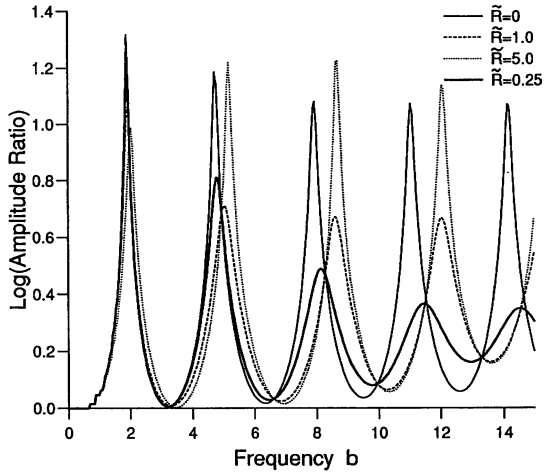

FIGURE 4 The frequency responses of the beam treated with an FSD element placed at $\Delta X = [0.0$–$0.1]$ for different values of the nondimensional viscous damping, $\widetilde{R}$, and for $C = I_f = 0$.

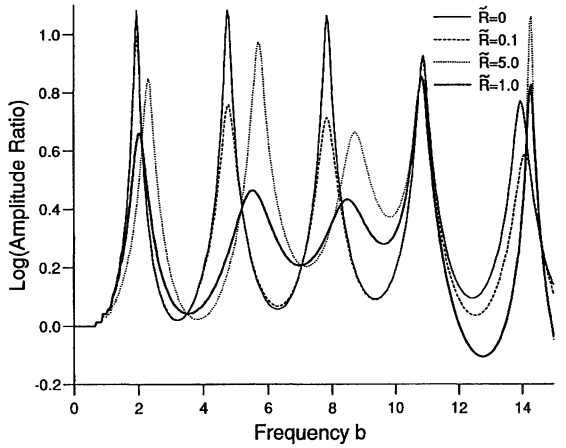

FIGURE 5 The frequency responses of the beam treated with an FSD element placed at $\Delta X = [0.0-0.2]$ for different values of the nondimensional viscous damping, $\tilde{R}$, and for $C = I_f = 0$.

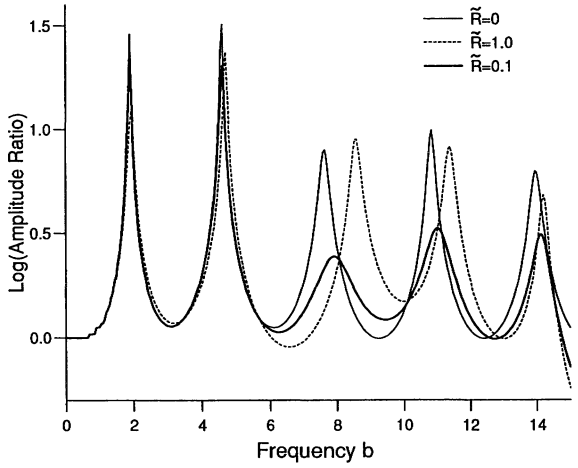

FIGURE 6 The frequency responses of the beam treated with an FSD element placed at $\Delta X = [0.2-0.4]$ for different values of the nondimensional viscous damping, $\tilde{R}$, and for $C = I_f = 0$.

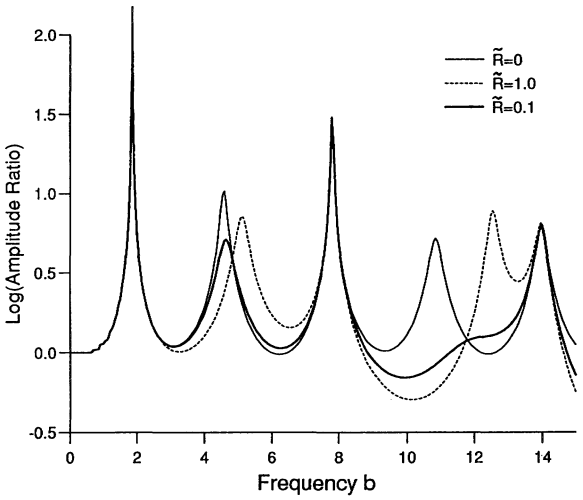

FIGURE 7 The frequency responses of the beam treated with an FSD element placed at $\Delta X = [0.4-0.6]$ for different values of the nondimensional viscous damping, $\tilde{R}$, and for $C = I_f = 0$.

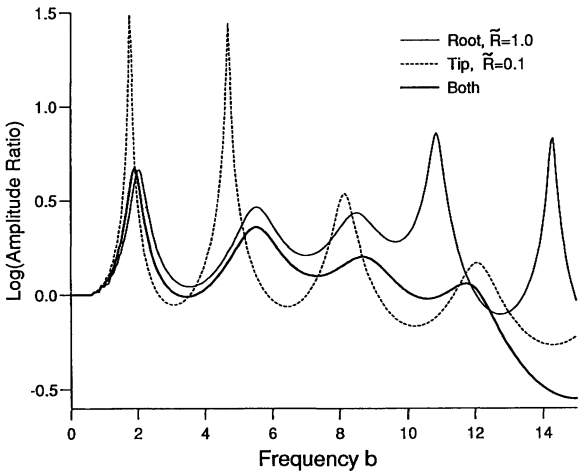

FIGURE 8 The frequency responses of the beam treated with two FSD elements placed at $\Delta X = [0.0-0.2]$ and $\Delta X = [0.7-0.9]$.

element results and the corresponding analytical ones, which are readily determined in terms of b. The values of α and μ roughly represent an aluminum beam ($E_1 = 70$ Gpa and $\rho_1 = 2700$ kg/m^3) with viscoelastic layers of Soundcoat DYAD 609 ($E_3^* \approx 700 + 700i$ Mpa and $\rho_2 = 1000$ kg/m^3), having approximately the same thickness of the beam. The choice of these materials is one of the options intended for the experimental work. However, it should be mentioned that the analysis conducted was qualitative and aimed at investigating a window within which the method is effective. Consequently, exact values of α and μ are not crucial at this stage of the analysis.

Damping Mechanism

It is useful to emphasize that the FSD treatment dissipates the excessive energy of the vibrating beam via two damping mechanisms.

1. Viscoelastic damping inherent in the surface layer material is proportional to the loss of Young's modulus of the viscoelastic material and to the strain energy captured by the surface layer. This is a reason why for best vibration suppression the layer should be placed at locations of high strain energy.

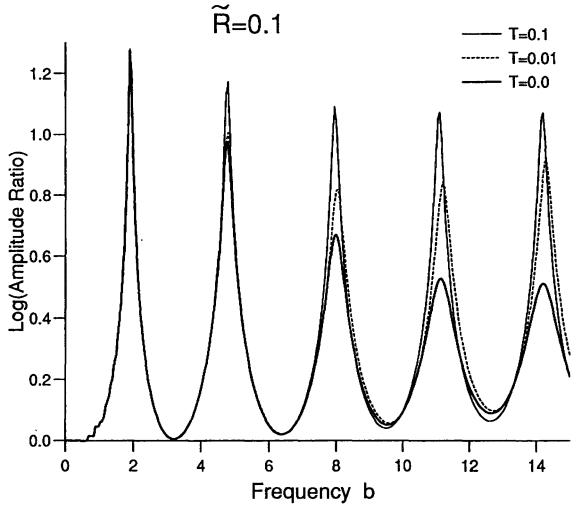

FIGURE 9 The frequency responses of the beam treated with an FSD element placed at $\Delta X = [0.0{-}0.1]$ for different values of the nondimensional hydraulic time constant, T, and for $\tilde{R} = 0.1$.

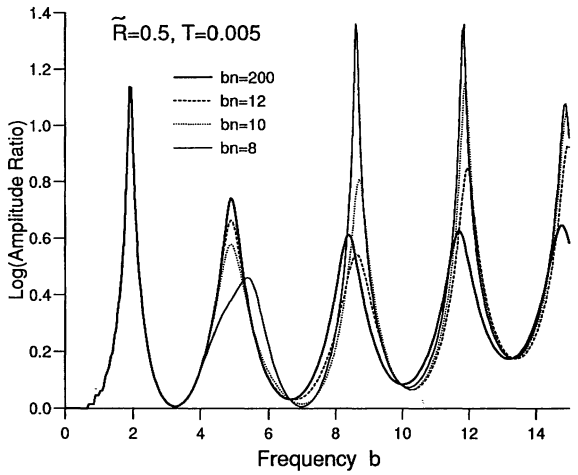

FIGURE 10 The frequency responses of the beam treated with an FSD element placed at $\Delta X = [0.0{-}0.1]$ for different values of the nondimensional frequency, bn, and for $T = 0.005$ and $\tilde{R} = 0.5$.

2. It can be shown that viscous damping emanating from the fluid flow through the passages, the energy dissipation per cycle, ΔE, is proportional to $\Delta\Theta^2$,

$$\Delta E = \int M_v \Delta\dot{\theta}\, dt$$
$$= i \int_0^{2\pi} Q^2 (K \otimes \Delta\theta)\Delta\theta\, d\omega t. \quad (12)$$

Consequently, for best performance at a given frequency of the FSD element, it should be placed such that the difference between the angular displacements, $\Delta\Theta$, at both ends of the element is maximum.

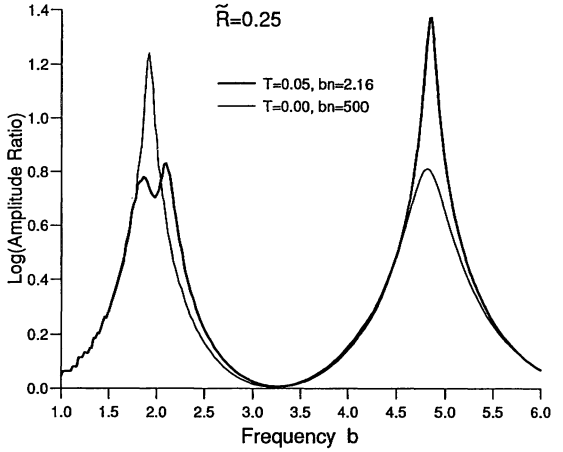

FIGURE 11 The frequency responses of the beam treated with an FSD element placed at $\Delta X = [0.0{-}0.1]$ and tuned to the first resonant frequency.

Effect of Viscous Damping. Figures 4–7 demonstrate the effect of $\tilde{R}$ on the frequency response of the beam treated with an FSD element of different lengths and placed at different locations. In all these figures the hydraulic capacitance, C, and inertance, I_f, are considered negligible. The figures indicate that for given location and length of the FSD element there is a range of $\tilde{R}$ that considerably reduces the peak vibration amplitudes over the frequency spectrum under consideration. Within this range, there is an optimum value of $\tilde{R}$, R^*, that suppresses the peak vibration amplitude(s) of a specific resonant frequency or frequencies the most. The higher the resonant frequencies, the smaller is the value of R^*, and vice versa. For example, an FSD element, with $L_b = 0.1$, placed at the vicinity of the clamping end (Fig. 4) achieves optimum damping at the third-to the fifth resonant frequencies when $R^* = 0.25$ and at the second resonant frequency when $R^* = 1.0$. Similarly, in Fig. 5 for $L_b = 0.2$, $R^* = 1.0$ more or less optimizes damping at the first three resonant frequencies while $R^* = 0.1$ is the optimum for the fifth resonant frequency.

Effect of Length and Location of FSD Element. The length of the FSD element affects the vibration suppression in two ways. As the length increases, the element captures and dissipates, via the viscoelastic damping mechanism, more strain energy. Consequently, the longer the FSD element, the more vibration suppression it provides. As the length increases, $\Delta\Theta$ changes and consequently the energy dissipation

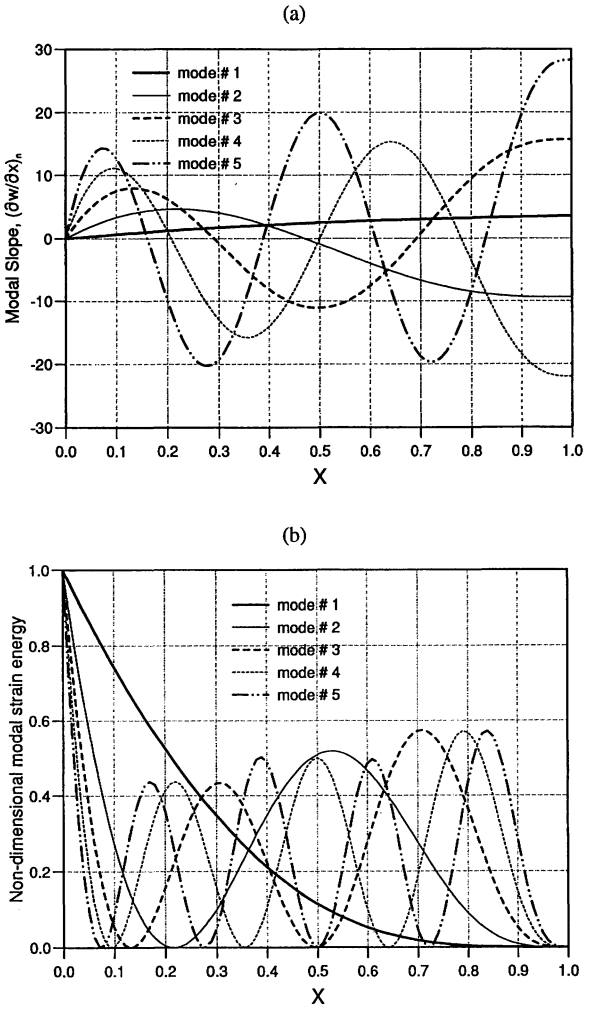

FIGURE 12 The first five nondimensional modal (a) Θ diagram and (b) strain energy diagram of a cantilever beam.

via viscous damping changes too. Because $\Delta\Theta$ may increase or decrease, vibration suppression of the peak vibration amplitudes may improve or deteriorate. The change in $\Delta\Theta$ at a given resonant frequency can be approximately predicted from the modal Θ diagram [Fig. 12(a)] as will be discussed next.

Figures 4 and 5 show the frequency response of the beam treated with FSD elements of different lengths located at the vicinity of the clamping end. When viscous damping is ignored ($\tilde{R} = 0$), the peak vibration amplitudes are reduced with increasing length of the FSD element, L_b. This is because of the increasing strain energy captured by the element, as depicted by the thin solid lines in Figs. 4 and 5. At R^* (thick solid lines), $\Delta\Theta$ is the major factor that controls vibration suppression. For $L_b = 0.1$, $\Delta\Theta$ increases with the increasing order of the resonant frequency [Fig. 12(a)], and consequently higher resonant peaks are suppressed more (Fig. 4). At $X = 0.2$, Fig. 12(a) shows that the fourth mode experiences a node; consequently viscous damping has little effect on the fourth resonant peak vibration amplitude when $L_b = 0.2$ as shown in Fig. 5.

Samples of the frequency responses of the beam treated with an FSD element having the a length $L_b = 0.2$ and placed at different locations are shown in Figs. 5–7. The axial locations presented are at $\Delta X = [0.0–0.2]$, $[0.2–0.4]$, and $[0.4–0.6]$, respectively. The effect of the location on the peak vibration amplitudes is also governed by the two damping mechanisms and consequently depends on the strain energy captured by the element and the value of $\Delta\Theta$. Viscoelastic damping via the surface layer becomes more effective when the FSD element is placed at locations of maximum strain energy and vice versa. The modal strain energy diagram is shown in Fig. 12(b) for the first five modes. Notice that the first modal strain energy (thick-solid line) is maximum at the clamping end and monotonically decreases with the increasing axial location, X. Consequently, in the absence of the fluid viscous damping ($R = 0$), the ability of the FSD element to suppress the first peak is maximum when the element is located at the base and is reduced as the element is located further away from the clamping surface. This abating vibration suppression ability is responsible for increasing the magnitude of the first peak as the FSD element is placed farther away from the clamping end (Figs. 5-7). Also, notice that at location 2, $\Delta X = [0.2–0.4]$, the second modal strain energy is small and the third is maximum. Consequently, viscoelastic damping reduces the second peak the least and the third the most as shown by the thin solid line ($R = 0$) in Fig. 6. The effect of $\Delta\Theta$ on the peak vibration amplitudes is demonstrated in Fig. 7 when the FSD element is placed at location 3, $\Delta X = [0.4–0.6]$. At this location $\Delta\Theta$ is minimum for the third and fifth modes and maximum for the fourth. Consequently $\tilde{R}$ has very little effect on the third and fifth peak vibration amplitudes, while when $\tilde{R} = 0.1$ the FSD treatment almost eliminates the fourth peak.

Clearly the effect of the FSD treatment on the vibration suppression of the beam is to some extent predictable, which facilitates the task of designing an efficient FSD treatment. From the modal Θ and strain energy diagrams, it can be predicted that a full treated beam will produce a good vibration suppression. A FSD element covering the entire length of the beam captures all the possible strain energy and renders high $\Delta\Theta$ for all modes. In addition to the nondesirable extra weight introduced by this treatment, the high length to diameter ratio of the fluid cavities will cause a violation of the uniform cavity pressure

assumption and render the present analytical model incorrect. An alternative efficient design may be accomplished by using multielements. A possible design is to use two elements located at the base, $\Delta X = [0.0-0.2]$, and near the tip, $\Delta X = [0.7-0.9]$. The frequency response of such a design is shown in Fig. 8. The responses due to each patch are also included as thin solid and dashed lines, respectively. The first patch effectively suppresses the first three peak vibration amplitudes and has little effect on the fourth and fifth peaks. The second patch, on the other hand, coincides with a near maximum $\Delta\Theta$ for the fourth and fifth modes [Fig. 12(a)] substantially reducing the corresponding peaks. This location, however, is virtually ineffective over the first and second modes. Using both patches produces a very effective vibration suppression over the entire spectrum as demonstrated by the thick solid line in Fig. 8.

Effect of Hydraulic Capacitance and Inertance. The effect of C and I_f are presented for the case when the FSD element is placed at the base and $L_b = 0.1$. Figure 9 displays the frequency responses for different values of T and when $I_f = 0$ and $\tilde{R} = 0.1$. Clearly, the effect of C is detrimental. As T increases, the peak vibration amplitudes across the spectrum increase. This effect is expected, because the volumetric flow through the connecting passages decreases as the compliance of the cavities increases (C increases), rendering less viscous energy dissipation. Similarly, the effect of the hydraulic inertance is in general detrimental. Figure 10 shows the effect of bn ($bn = \sqrt{\Omega_n}$) on the frequency response for the case when $\tilde{R} = 0.5$ and $T = 0.005$. Notice that as Ω_n decreases, I_f increases and the effect of the inertance becomes more pronounced. Some limited improvement, however, can be accomplished for a given combination of R, C, and I_f where the peak vibration amplitude can be reduced at one or two frequencies at the expense of a pronounced increase at the other frequencies.

It should be pointed out that when C and I_f are significant, the FSD element can be used as a damped absorber and tuned to suppress a specific peak vibration amplitude. Figure 11 demonstrates the effect of the FSD element on the frequency response of the beam when R, C, and I_f are tuned to the first natural frequency ($bn = 2.16$). Clearly, a considerable suppression of the peak is achieved. However, this improvement is at the expense of the response at the second resonant frequency.

CONCLUSION

A simple and passive technique for the vibration suppression of beamlike structures is proposed where two viscoelastic surface layers with connected fluid-filled cavities are attached to the opposite surfaces of the beam. In addition to the viscoelastic damping of the surface layers, the technique provides viscous damping due to the fluid flow through the connecting passages. A mathematical model of a FSD-treated cantilever beam is developed and solved. A parametric study is conducted to investigate and assess the effectiveness of the technique. The investigation reveals the following.

1. Best performance (vibration suppression) of the method is attained under the following condition:
   - an optimum value of the flow-through-passage viscous resistance;
   - negligible hydraulic capacitance and inertance; and
   - the length and location of the FSD element are such that it captures the maximum strain energy, and the difference between the angular displacements at both ends of the element is maximum.
2. With two elements attached at the base and near the tip of the beam, all peak vibration amplitudes over the entire frequency domain studied can be well suppressed.
3. The effect of the hydraulic capacitance and inertance are, in general, detrimental. However, for certain values, the FSD element acts as a damped absorber and can be tuned to suppress the vibration at a specific frequency.

In brief, the investigation showed that the proposed technique has promising potential in the field of vibration suppression of beamlike structures. Experimental work to bolster the current claim will be conducted.

REFERENCES

Agnes, G. S., and Napolitano, K., 1993, "Active Constrained Layer Viscoelastic Damping," *Proceedings of the 34th SDM Conference*, pp. 3499–3506.

Baz, A., and Ro, J., 1993, "Active Constrained Layer Damping," *Proceedings of Damping 93*, San Francisco, CA, pp. IBB 1–23.

Baz, A., and Ro, J., 1994, "Performance Characteristics of Active Constrained Layer Damping," *Shock and Vibration*, Vol. 2, pp. 33–42.

Christenen, R. M., 1982, *Theory of Viscoelasticity: An Introduction*, 2nd ed., Academic Press, New York.

Cremer, L., Heckle, M., and Ungar, E., 1988, *Structure-Borne Sound: Structural Vibrations and Sound Radiation at Audio Frequencies*, Springer-Verlag, Berlin.

Dosch, J. J., Inman, D. J., and Garcia, E., 1992, "A Self-Sensing Piezoelectric Actuator for Collocated Control," *Journal of Intelligent Materials, Systems, and Structures*, Vol. 3, pp. 166–185.

Ghoneim, H., 1995, "Application of the Electromechanical Surface Damping to the Vibration Control of a Cantilever Plate," *Journal of Sound and Vibration*, to appear.

Hagood, N. W., and Von Flotow, A., 1991, "Damping of Structural Vibrations with Piezoelectric Materials and Passive Electrical Networks," *Journal of Sound and Vibration*, Vol. 146, pp. 243–268.

Harrison, J. C., Imanio, W., and Talke, F. E., 1994, "Tuned Constrained Layer Damping of a Cantilever Plate," *Journal of Sound and Vibration*, Vol. 174, pp. 413–428.

Henze, D., Karam, R., and Jeans, A., 1990, "Effect of Constrained-Layer Damping on the Dynamics of a 4 In-Line Head Suspension," *IEEE Transactions on Magnetics*, Vol. 26, pp. 2439–2441.

Hollkamp, J. J., and Starchville, T. F., Jr., 1994, "Self-Tuning Piezoelectric Vibration Absorber," *Journal of Intelligent Materials, Systems, and Structures*, Vol. 5, pp. 559–566.

Ingard, K. U., and Akay, A., 1987, "On the Vibration Damping of a Plate by Means of a Viscous Fluid Layer," *ASME Journal of Vibration, Acoustics, and Reliability in Design*, Vol. 109, pp. 178–184.

Liao, C. Y., and Sung, C. K., 1991, "Vibration Suppression of Flexible Linkage Mechanisms Using Piezoelectric Sensors and Actuators," *Journal of Intelligent Materials, Systems, and Structures*, Vol. 2, pp. 177–197.

Nashif, D., Jones, D. I. G., and Henderson, J. P., 1985, *Vibration Damping*, Wiley, New York.

Nostrand, V., Knowles, W. C., and Inman, D. J., "Active constrained Layer Damping for Micro-Satellites," in C. L. Kirk and P. C. Hughes, *Dynamics and Control of Structures in Space*, Vol. II, 1993, pp. 667–681.

Onsay, T., 1994, "Dynamic Interaction Between the Bending Vibrations of a Plate and a Fluid Attenuator," *Journal of Sound and Vibration*, Vol. 178, pp. 289–313.

Rahn, D. C., and Joshi, S., 1994, "Modeling and Control of an Electrorheological Sandwich Beam," *ASME Active Control of Vibration and Noise*, Vol. DE-75, pp. 159–167.

Reddy, J. N., 1993, *An Introduction to the Finite Element Method*, 2nd ed., McFraw–Hill, New York, pp. 147–150.

Shen, I. Y., 1994, "Bending-Vibration Control of Composite and Isotropic Plates Through Intelligent Constrained-Layer Treatments," *Smart Materials and Structures*, Vol. 3, pp. 59–70.

Tomlinson, G. R., 1990, "The Use of Constrained Layer Damping in Vibration Control," *International Journal of Mechanical Sciences*, Vol. 23, pp. 233–242.